https://doi.org/10.31436/iiumej.v25i2.2964

A STUDY ON THE TERRESTRIAL MOBILITY OF A SPHERICAL AMPHIBIAN ROBOT

MOHD BAZLI BAHAR[1,2,3]*, SHAHRUM SHAH ABDULLAH[2], MOHD SHAHRIEEL MOHD ARAS[1,3], MOHAMAD HANIFF HARUN [1,3], MUHAMAD KHAIRI ARIFIN[1], FARIZ ALI@IBRAHIM[1]

[1]Fakulti Teknologi dan Kejuruteraan Elektrik, Universiti Teknikal Malaysia Melaka, Hang Tuah Jaya, 76100 Durian Tunggal, Melaka, Malaysia
[2]Department of Electronic Systems Engineering, Malaysia-Japan International Institute of Technology, UTM KL Campus, Jalan Sultan Yahya Petra, 54100 Kuala Lumpur, Malaysia
[3]Underwater Technology Research Group (UTeRG), Center for Robotics and Industrial Automation (CERIA), Fakulti Kejuruteraan Elektrik, Universiti Teknikal Malaysia Melaka, 76100 Durian Tunggal, Melaka, Malaysia.

**Corresponding author: mohdbazli@utem.edu.my*

(Received: 17 August 2023; Accepted: 9 January 2024; Published online: 15 July 2024)

ABSTRACT: Amphibian spherical robots are an appealing and practical alternative that can move around on different surfaces and function in aquatic environments. Spherical robots boast remarkable mobility and robustness, enabling them to navigate and perform exploration and reconnaissance tasks even in challenging or harsh environments. This paper explores assessing the terrestrial travel capabilities of a proposed amphibian spherical robot. A rapid Prototyping machine (RPM) was used to print the prototype's main shell, yoke, and circuit holders. One main circuit was built on the yoke, while the other was positioned in the bottom shell. The driving principle used the barycentre offset notion, in which a pendulum mass is used to vary the location of the mass to generate a motion. Additional mass is added to the pendulum to determine the robot's performance when mass is altered. The results reveal that the robot can travel on land with a maximum velocity of 40.75 degrees per second while carrying 600 grams of weight and a turning angle of 22.8 degrees. The robot can only move when the additional mass exceeds 400 grams.

ABSTRAK: Robot sfera amfibia ialah satu alternatif menarik dan praktikal yang dapat bergerak di atas permukaan berbeza dan berfungsi dalam persekitaran akuatik. Robot sfera mempunyai mobiliti yang luar biasa dan tahan lasak. Ciri ini membolehkannya bergerak dan menjalankan tugas penerokaan dan peninjauan dalam persekitaran merbahaya atau buruk. Kajian ini adalah bagi menganalisis prestasi robot sfera amfibia ketika bergerak di darat. Mesin Pemprototaip Pantas (RPM) digunakan bagi mencetak badan utama prototaip, yok, dan pemegang litar. Satu litar utama dibina pada yok, manakala satu lagi diletakkan di bahagian bawah. Prinsip pemanduan adalah dengan menggunakan konsep penentuan kedudukan pusat jisim, di mana jisim pendulum digunakan bagi menentukan lokasi jisim sambil menghasilkan gerakan. Berat tambahan pada jisim pendulum ditambah bagi mendapatkan prestasi robot apabila jisim diubah. Dapatan kajian menunjukkan robot dapat bergerak atas darat dengan halaju maksimum 40.75 darjah sesaat sambil membawa 600 gram berat dengan sudut pusingan sebanyak 22.8 darjah. Robot hanya boleh bergerak apabila tambahan jisim melebihi 400 gram.

KEYWORDS: *spherical robot, terrestrial motion, pendulum*

https://doi.org/10.31436/iiumej.v25i2.2964

1. INTRODUCTION

The earth's surface has various structures like hills, cliffs, lakes, and rivers. The sea is said to cover 71% of the earth's surface [1]. In finding or collecting earth resources, workers face various problems, primarily related to safety [2-3]. Besides, the earth is often plagued by natural disasters [4-5]. Search and rescue tasks should be done as soon as possible and carried out safely for the rescuer and the victim. Therefore, a robotic system capable of carrying out activities to locate and collect resources and be used as a first responder when disasters occur is crucial [6]. These robots need to be equipped with the ability to move around on various surfaces and operate in watery areas. Besides, the robot's durability must also be emphasized to ensure it can successfully perform its task.

One attractive and practical solution to these issues is using a spherical robot. A spherical robot motion is based on the rolling concept inspired by the pangolins [7]. This locomotive mode is faster and safer as its spherical body becomes a protective shield. A spherical robot has high mobility and is robust against its surrounding environments [8], which allows it to perform exploration and reconnaissance tasks in unfriendly or harsh environments [9]. Furthermore, spherical robots are naturally stable and can recover from collisions [7]. They also can conceal and protect all the essential parts inside the sphere against environmental states such as moisture, radiation, dust, hazardous material, or water pressure [10]. The steering hydrodynamic force can be reduced as the robot is spherical, increasing movement flexibility [3]. Combining different driving mechanisms makes the robot amphibious, meaning it has terrestrial and aquatic abilities. The major challenge is mass distribution as it has a round shape nature [11]. Furthermore, limited physical size and compact structure require an optimal actuator for both conditions [12]. Therefore, a suitable driving principle is crucially needed to cater to both the design constraints and maneuverability.

An amphibian spherical robot commonly combines terrestrial and underwater driving principles. To optimize the actuation, both driving principles are set to work together, especially when operating underwater [3,13-14]. The terrestrial drive units control thrust direction to improve the system's maneuverability. Applying a legged actuator to move on land and underwater is another solution to cater to the maneuverability of an amphibian spherical robot [15-17]. Still, the design has more actuators, and complex motion planning is needed.

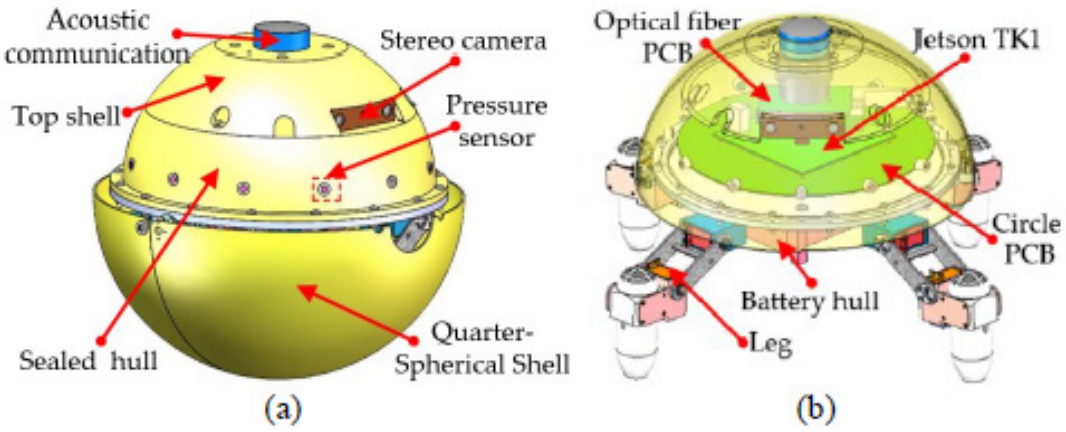

Fig. 1. The legged design proposed in [15] where 4 legs were used as actuators to move on terrestrial and a water jet was installed at the tip of the legs to provide thrust when traveling underwater.

Therefore, a novel amphibian robot was developed to reduce complexity while taking design restrictions and maneuverability into account. The research investigates the assessment of a proposed amphibian spherical robot's terrestrial travel capabilities in terms of motion pattern, turning angle, and motion velocity.

2. THEORETICAL BACKGROUND

Several driving principles have been found, generally divided into three (3) different types. These include methods that move the robot's center of mass (barycenter offset), methods that rely on changing the spherical shell's shape, and methods that generate variable gyrostatic momentum [18]. From this three-basis method, a combination of any one of these was also proposed [19]. The barycenter offset involves shifting the mass location within the sphere from one point to another. This necessitates integrating moving components within the sphere, which can take the form of a cart, pendulum, or slider [8]. Among these options, the rotating pendulum method is a prevalent choice in prior research endeavors. The design has at least two drive motors; one is used to roll the yoke, while another is used to control the pendulum angle [11,20-26].

However, Spherical robots driven by a pendulum method produce less force for the sphere to move. The problem can be reduced by adding more pendulums inside it, but the space is limited. A wheel fixed to the spherical shell was proposed to minimize this issue. The wheel is driven by a motor and placed on a yoke at the sphere's center [23].

Masses can be used as propulsion by swinging the pendulum or moving the masses straight from the sphere's center to its surface. Slippage does not occur for this method because no mass is in contact with the spherical surface. The amount of energy produced depends on the weight of the mass used. The mobility of this method can be improved by adding mass to the robot. Up to 4 pendulum units are used to move in all axes, increasing the robot's motion torque. However, the increasing number of pendulums will also increase the robot's weight and control method complexity so that it can perform a stable motion.

2.1. Barycenter offset

The barycenter offset driving principle implemented in the spherical robot applied several methods. A pendulum is one of the common ways to change the mass location inside the sphere. K. Landa and A.K. Pilat describe the dynamic of such a system using the Lagrange Eq. (1), where U_1 is the potential energy of the sphere with respect to its centroid, U_2, the potential energy of the pendulum with respect to the sphere's centroid, K_1, the kinetic energy of the sphere, K_2, the kinetic energy of the pendulum, T_1, the rotational energy of the sphere, and T_2 represents the rotational energy of the pendulum [27]. The model assumes that the system is a two rigid-body system with a single degree of freedom between them.

$$L = K_1 + K_2 + T_1 + T_2 - U_1 - U_2 \tag{1}$$

Based on Eq. (1), K. Landa and A.K. Pilat state in [28] that the transfer function that shows the relationship between the sphere inclination angle and pendulum angle as Eq. (2). $L_1(s)$ is the Laplace transform of the sphere inclination angle, $L_2(s)$ is the Laplace transform of the pendulum angle, and T_v is the coefficient of viscous friction.

$$\frac{L_1(s)}{L_2(s)} = \frac{(A_2 - 2A_3)^2 - 2A_4}{(A_1 - 3A_2 + A_3)s^2 - T_v s + 2A_4} \tag{2}$$

https://doi.org/10.31436/iiumej.v25i2.2964

Where

$A_1 = J_1 + J_2 + M_1R^2 + M_2R^2 + M_2l^2$

$A_2 = M_2Rl$

$A_3 = J_2 + M_2l^2$

$A_4 = M_2gl$

$J1$ – moment of inertia of the sphere around its centroid,
$J2$ – moment of inertia of the pendulum around the sphere's centroid,
M_1 – mass of the sphere,
M_2 – mass of the pendulum,
g – acceleration of gravity
R – sphere radius
l – pendulum length

From the transfer function, the position or sphere rotation depends on the moment of inertia of the pendulum. This is valid when the sphere's initial center of mass is aligned with the pendulum's origin. Therefore, the mass distribution inside the sphere must be equal on each side to ensure the pendulum motion can change the sphere orientation.

2.2. Static Equilibrium

An object with mass has inertia that is determined by the mass energy exerted on it [29]. This inertia will keep the object at its original state until external forces are given. The body is in static equilibrium if every material point in a body has the same constant velocity relative to an inertial system [30]Stefan Lindstrom states that a body's static equilibrium occurs when the force-couple system acting on it is a zero system. This means that the force and moment sum of the force-couple systems equals zero, as in Eq. (3).

$$\begin{aligned} \sum F_x = 0,\ \sum M_{Ax} = 0, \\ \sum F_y = 0,\ \sum M_{Ay} = 0, \\ \sum F_z = 0,\ \sum M_{Az} = 0, \end{aligned} \tag{3}$$

3. METHODOLOGY

As indicated in Fig. 2A spherical robot was developed to test the proposed driving principle. A complete overview of the mechanical design was discussed in [31]. The proposed spherical robot electronic circuit was located on the yoke to control the terrestrial actuator and main sphere sensory unit. A secondary electronic circuit was used to control the underwater actuator and sensory situated at the bottom of the lower casing.

Two units of inertial measurement unit (IMU) were used to detect the yoke and the sphere motion. All the data was gathered by a raspberry located in the yoke. Additionally, the yoke controls all the actuators located on the yoke, while the secondary circuit controls the actuator for the underwater motion.

https://doi.org/10.31436/iiumej.v25i2.2964

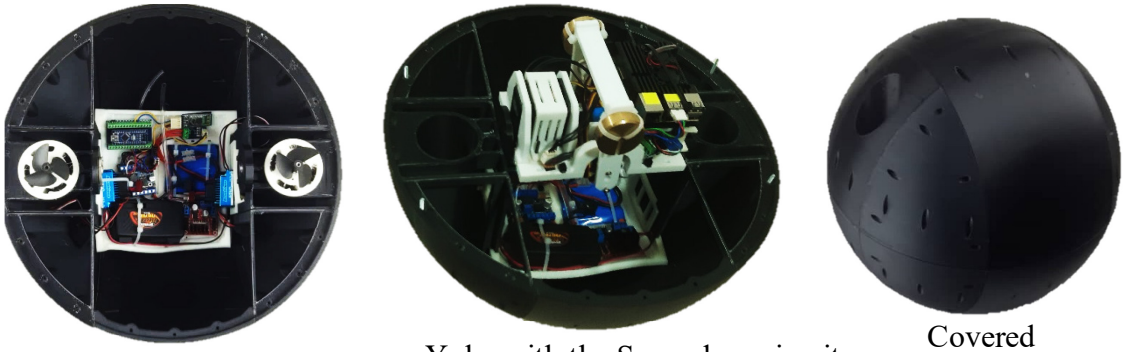

Secondary circuit assembly | Yoke with the Secondary circuit | Covered

Fig. 2. Proposed design (Left: the secondary circuit assembly with the lower cover. Center: Assembly of the secondary circuit with the Yoke. Right: Top cover was installed to the proposed design).

3.1. A proposed terrestrial driving principle

The proposed design rolled on a pitch by changing the yoke angle, while the sphere roll angle was manipulated by swinging the pendulum. The pendulum was placed on top of the yoke, as in Fig. 2 to increase the offset mass inside the sphere. Detailed discussion regarding the proposed driving principle is in [32].

The proposed movement must be tested for its effectiveness in terms of moving, turning, and determining motion velocity with various settings. This information is necessary to obtain the optimum calibration for the robot before developing a suitable control system. Furthermore, experiments must be performed to establish the proposed robot's limitations.

3.2. Experimental Procedures

The experimental procedures began with the initial setup, a step adopted across all experiments to ensure data consistency. Subsequently, a detailed description of the testing methodology is provided.

3.2.1 Initial Setup

The procedure begins with the initialization of the yoke and pendulum angle. To ensure that the robot center is perpendicular to the ground, spirit level was used to measure the position while the yoke angle, θ_Y and pendulum angle, θ_P is tuned to identify the initial θ_{Yi} and θ_{Pi}.

From the pendulum's initial angle θ_{Pi}, the maximum angle to the left and right was identified. To do so, six (6) pieces of weight coin were attached to the pendulum as depicted in Fig. 3. 600g is the maximum mass that can be added to the pendulum due to the limited space. The tuning was done in this setup to ensure a consistent angle can be used for different added mass. From the test, the pendulum can rotate 7^0 to the left and right. Therefore, for 500g to 600g added mass, three pendulum angles, θ_P is tested, which is -7^0 , 0^0, and 7^0.

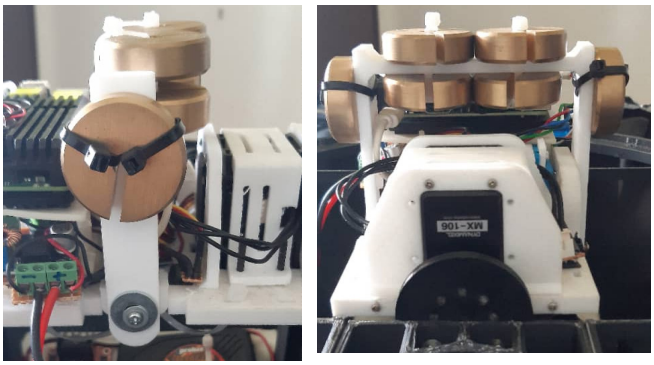

Fig. 3. A total of 600g (6 pieces) added mass attached to the pendulum.

Secondly, the environment was set as depicted in Fig. 4. The total test area is $3.25m^2$ and the same material was used for all the tests done. The start and center lines were marked on the test area to ensure the initial position was consistent.

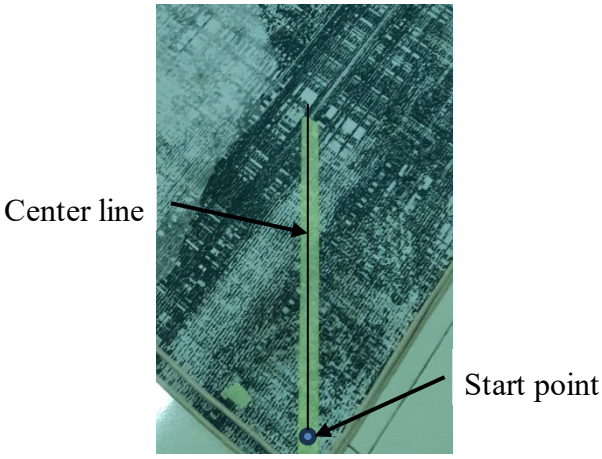

Fig. 4. Environment setup for the experiment.

3.2.2 Performing the Experiment

1. The proposed robot was placed on top of the Start point and aligned with the initial line by measuring the front and back of the robot using a spirit level, as in Fig. 5.

Fig. 5. Setting the initial position of the proposed robot.

2. The pendulum angle was set at 0 degrees with a 500g mass placed on it.

3. The motion was observed to identify the first and second cycles. At the end of each cycle, a mark was made on the floor to represent each completed cycle.

4. The angle of each cycle was measured based on the angle between the center line with a straight line to the cycle point.

5. Distance was measured from the start to the first cycle point, and from the first cycle point to the second. Fig. 6 shows the measured method.

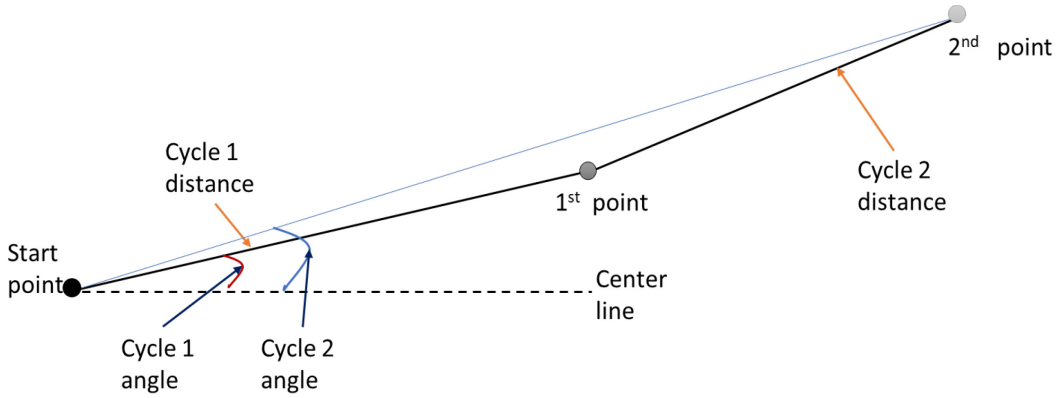

Fig. 6. Method to measure the data.

6. Step 1 until 5 was repeated 5 times.

7. Step 1 until 6 was repeated with pendulum angles of +7 and -7 degrees.

8. Step 1 until 7 was repeated with a 600g pendulum mass.

9. By installing the propeller to the proposed robot, steps 1 until 6 were repeated to observe the motion difference when the proposed robot mass increased.

The procedure was done to prove that the proposed driving principle can drive the proposed robot from one point to the other. Furthermore, the experiment was able to identify the maximum turning angle of the proposed robot. Fig. 7 represents the flowchart of the experiment procedure for a 500g mass located at the pendulum. The procedure was repeated with a 600g mass, followed by the installation of propellers with a 600g mass.

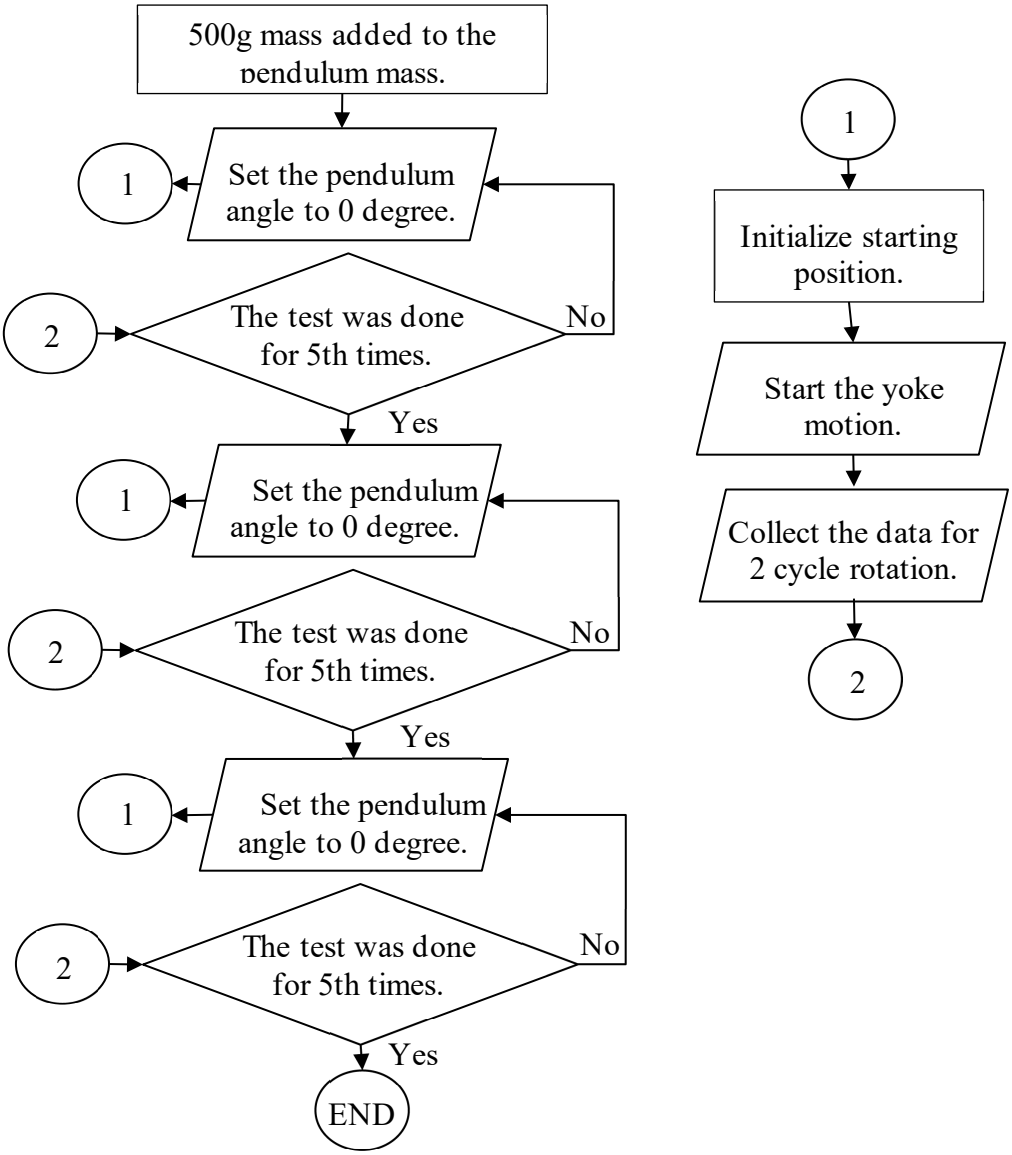

Fig. 7. Flowchart of the experiment procedure for 500g mass. The same step was used for 600g mass.

4. RESULTS AND DISCUSSIONS

The proposed spherical amphibian robot can travel on a dry surface with a minimum $30.84°/s$ and a maximum of $40.75°/s$. The average roll velocity for each test done is in Table 1.

Table 1: Average velocity of the proposed system when traveling on land.

Mass	Average Velocity (degree/second)	
	Cycle 1	Cycle 2
500g	32.97	39.21
600g	36.81	40.75
600g with propeller	30.84	32.79

Analyzing the velocities of the first and second cycles reveals that the system achieves its highest speed when bearing a weight of 600g. Notably, the second cycle consistently exhibits

https://doi.org/10.31436/iiumej.v25i2.2964

greater speed across all trials than the first. This phenomenon is attributed to the momentum acquired during the initial cycle being transferred to the subsequent one. In the initial cycle, the system contends with inertia, thereby impeding acceleration. Notably, the system experiences increased inertia when engaging the underwater circuit, resulting in reduced velocity.

Fig. 8 depicts the roll motion data for three distinct pendulum locations, with the top figure representing the roll angle of 7° to the left, the middle figure representing 0 degrees, and the bottom figure representing 7° to the right. The y-axis is the angle data provided by the IMU sensor while the step in the x-axis represents the time data was taken (loop time).

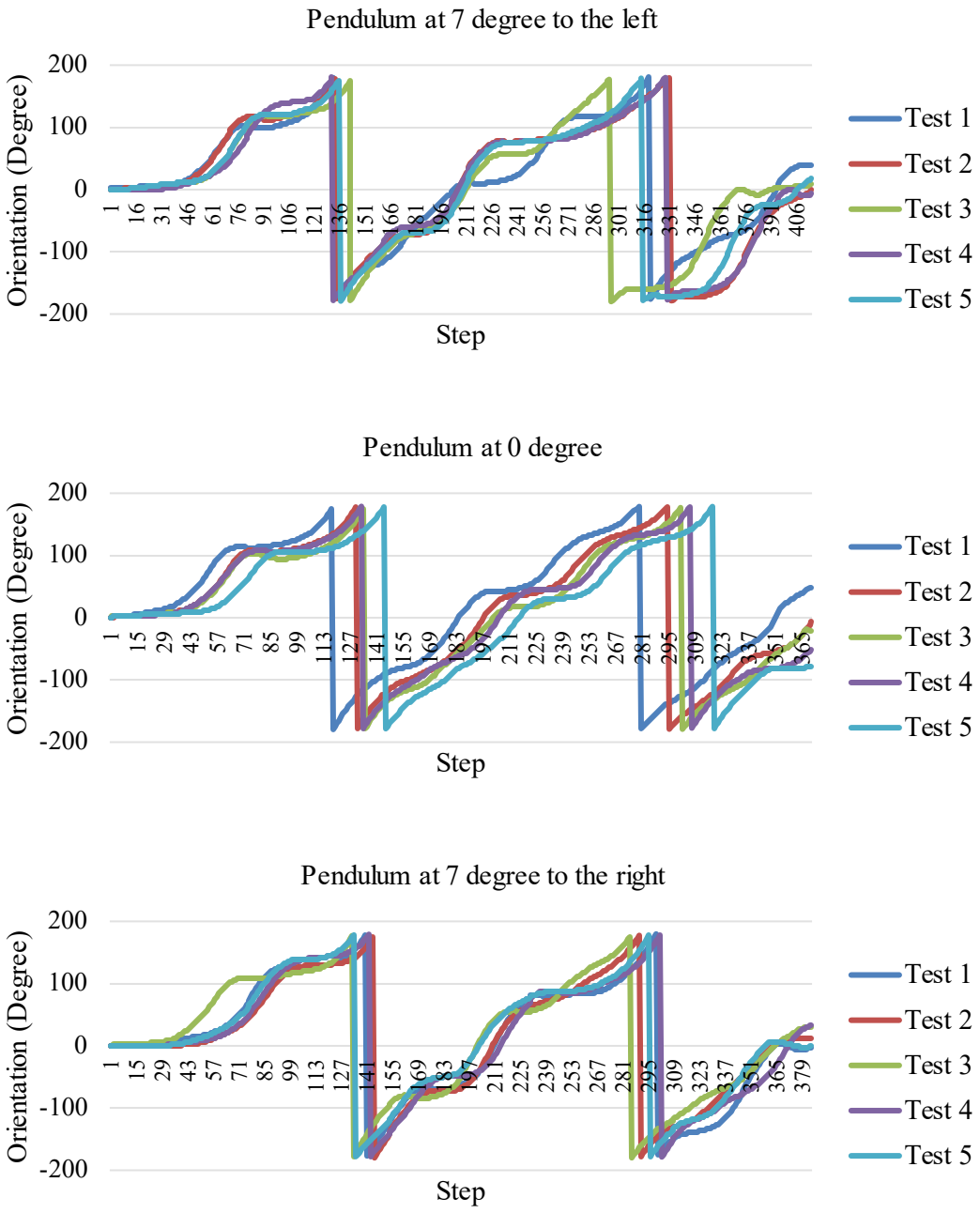

Fig. 8. Roll motion of the proposed system.

https://doi.org/10.31436/iiumej.v25i2.2964

Based on the roll angle obtained, the roll movement pattern was the same for all three pendulum locations. When the proposed system was in motion, the change in velocity was caused by the presence of a secondary circuit in the proposed system, causing the change in CoM to become uneven. This caused the system to decelerate temporarily until the yoke could overcome the secondary circuit mass. Fig. 9 depicts the relationship between angular velocity and the rolling motion of the proposed system, where the top graph shows the system's rolling together with the yoke motion (black line). In contrast, the graph at the bottom depicts the angular velocity profile.

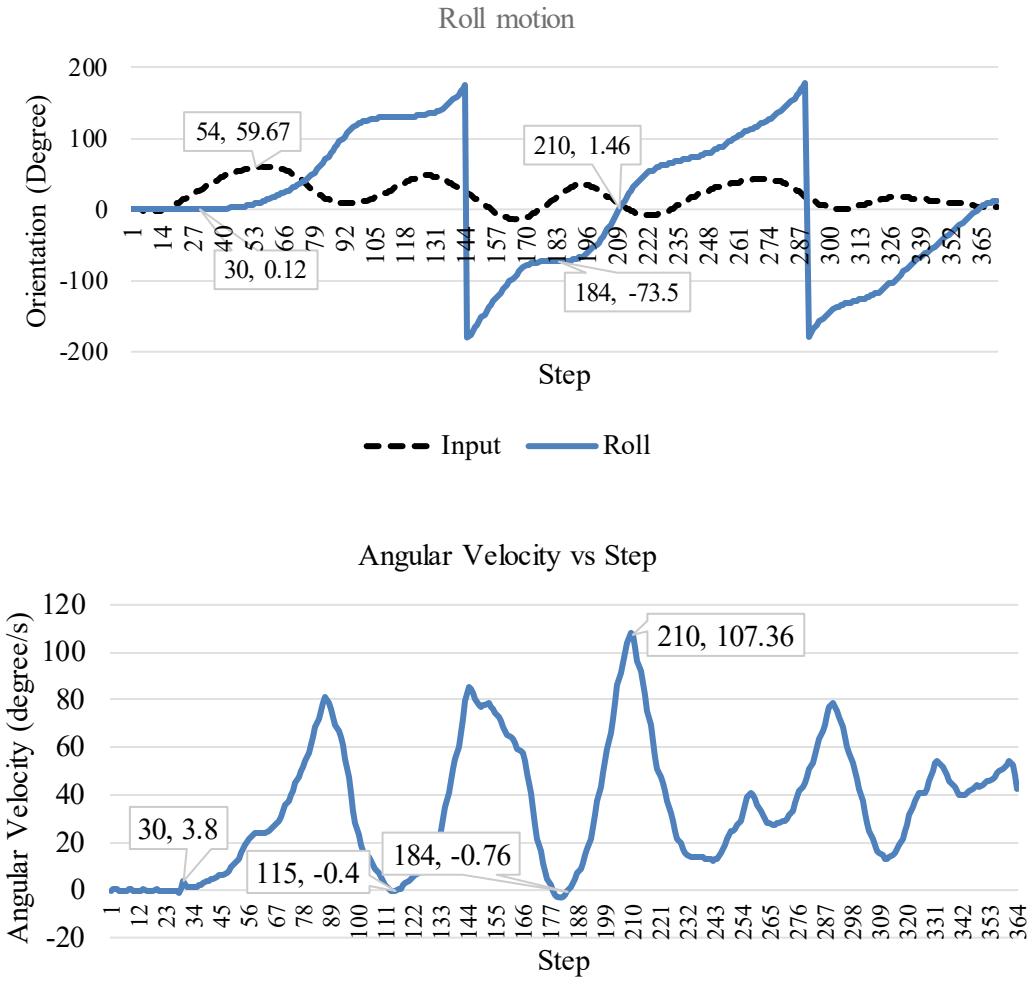

Fig. 9. Roll and angular velocity of the proposed system.

Fig. 10 depicts the pitch angle of the proposed system gathered from the secondary circuit's sensor readings. Each graph, like Fig. 8, illustrates a distinct position of the pendulum.

https://doi.org/10.31436/iiumej.v25i2.2964

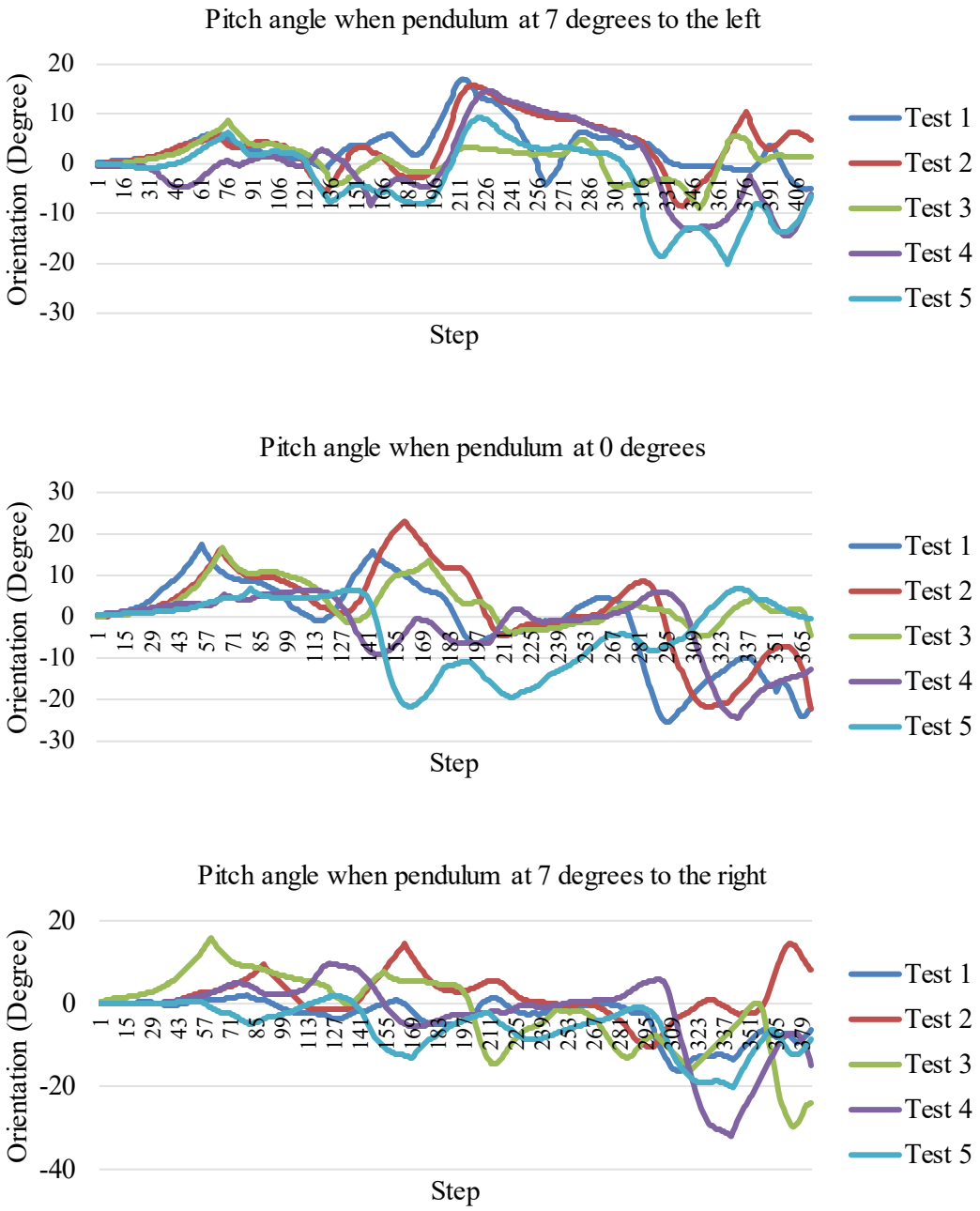

Fig. 10. Pitch motion of the proposed system.

Based on the pitch angle data, the suggested system consistently demonstrates lateral movement to the left and right. However, this behavior is not uniformly observed across all experiments for the three pendulum positions. The system initially exhibits a stable pattern that gradually becomes unstable over time. This transition can be attributed to the absence of a controlling mechanism throughout the testing phase, allowing the mounting momentum to impact the system's motion progressively. The system's average turning motion is depicted in Fig. 11.

https://doi.org/10.31436/iiumej.v25i2.2964

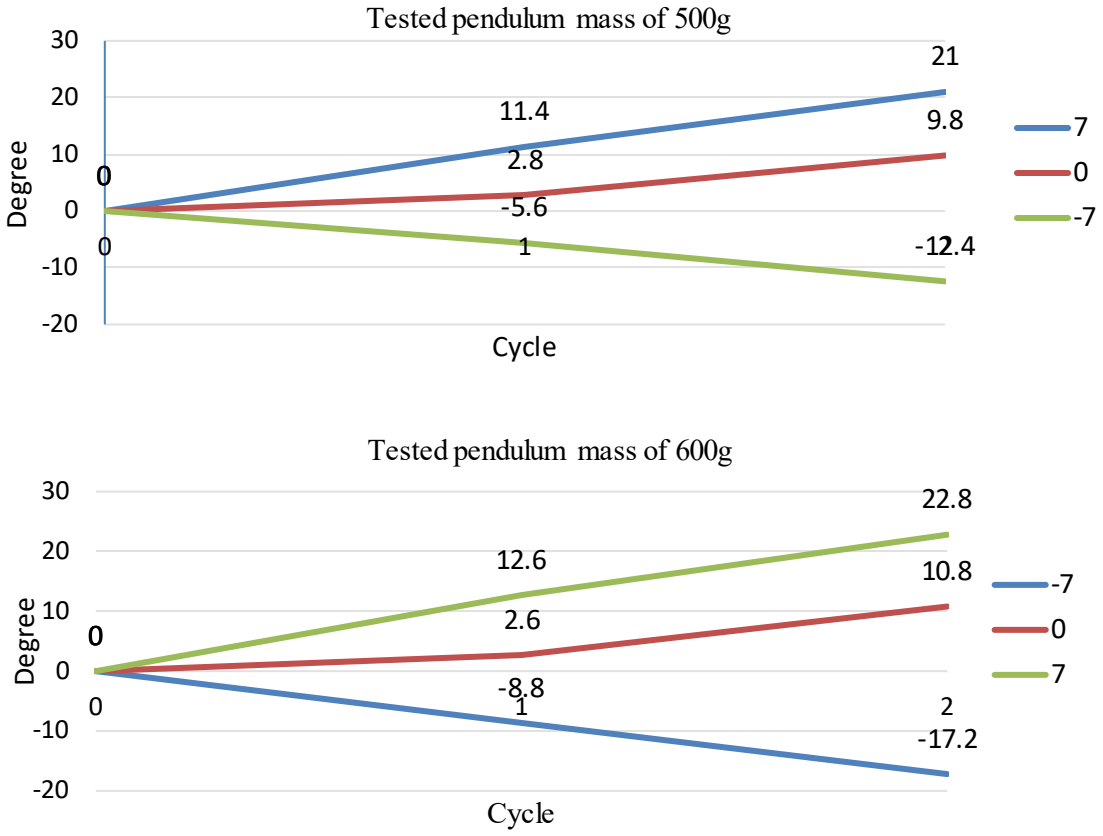

Fig. 11. Turning angle of the proposed system.

Due to the constraint of the pendulum movement, which can only travel 14 degrees, the proposed system requires a significant distance to turn. Based on the results, the maximum turning for the first cycle is 12.6 degrees, and the maximum turn for the second cycle is 22.8 degrees when 600g of weight is applied. On average, adding weights can increase the degree of rotation by 1.53 degrees in the first cycle and 2.53 degrees in the second cycle.

Fig. 12 depicts the distance traveled by the system during the first and second cycles with weights of 500g (top) and 600g (bottom). The longest distance is shown in the test that placed the pendulum in the middle (0 degrees), which is 212.64 cm, while changing the pendulum's angle minimizes the system's travel distance.

Fig. 13 represents the rolling motion of the proposed system (OUTPUT) when a 400g mass is added. While the yoke (INPUT) rolled to 90^0, the system is still in its position because the force created by the yoke motion is insufficient to encounter the inertial moment. Compared to the graph in Fig. 9 (top), the system started to roll before the yoke rolled to 90^0. Therefore, the mass needed to flee from the static equilibrium must be greater than 1113.8g, whereas 713.8g came from the yoke and pendulum, with an additional 400g added to the pendulum. The limitation of space inside the sphere limits the number of weight coins that can be placed at the pendulum. The increasing number of weight coins will decrease the pendulum rotation angle.

https://doi.org/10.31436/iiumej.v25i2.2964

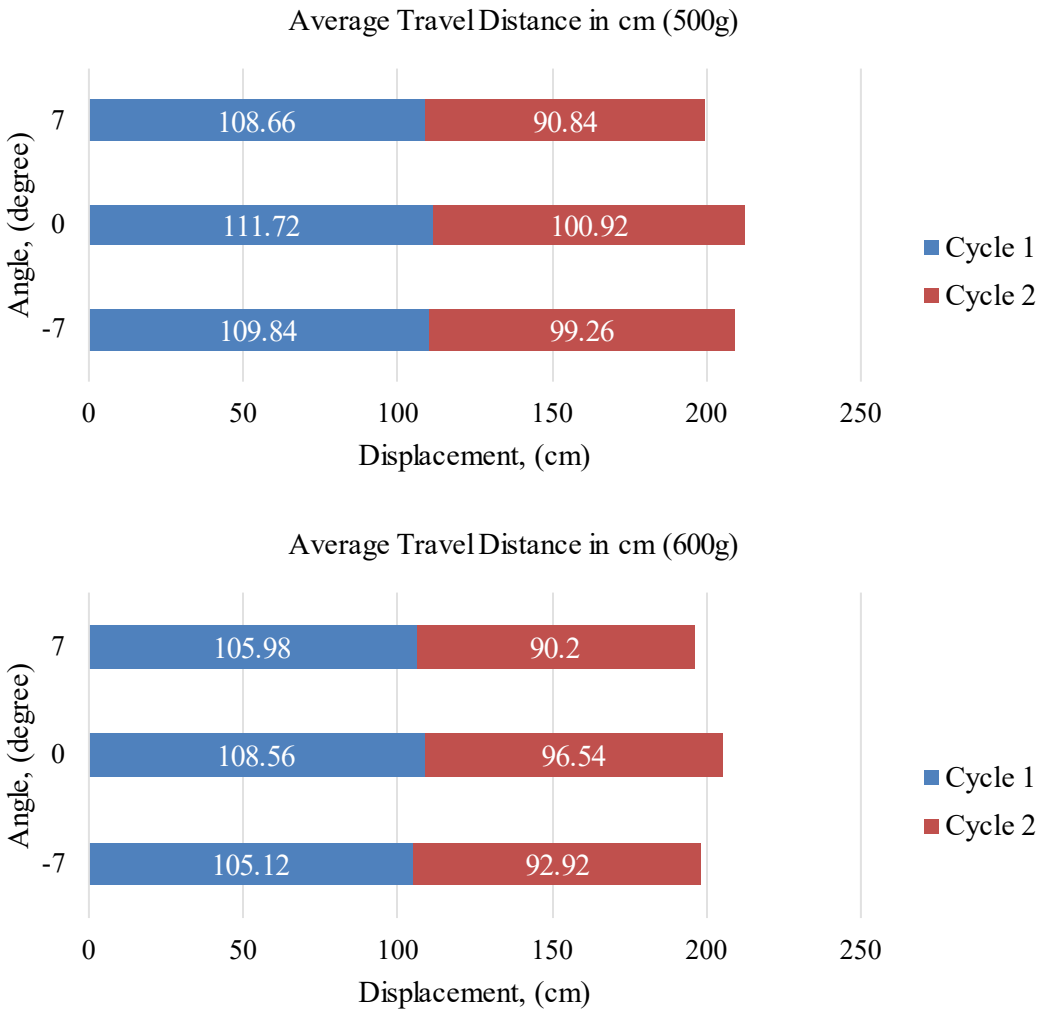

Fig. 12. Displacement of the proposed system.

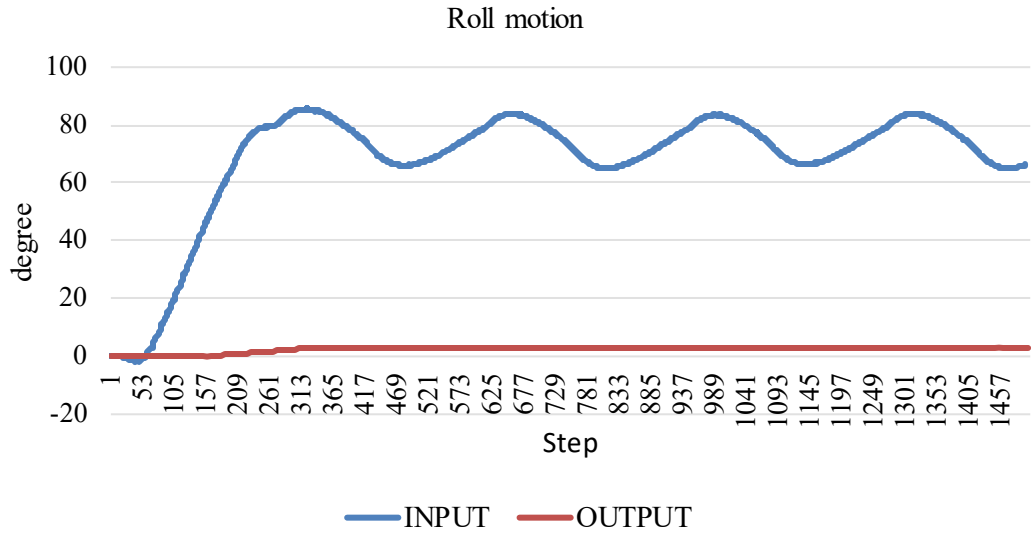

Fig. 13. Roll motion of yoke and the proposed system.

5. CONCLUSIONS

The proposed spherical amphibian robot can travel on a dry surfaces with a maximum velocity of 40.75 degree/s while carrying 600g of mass. It needs more than 400g of additional mass to encounter inertia to move. From the experiment, the increasing mass of the pendulum increases the velocity and turning angle of the proposed system. The propeller with its motor and drivers (549g) was excluded from the experiment so that the weight may be varied to two values, 500g, and 600g. The robot's roll motion remains consistent across all experiments, while its yaw motion varies. This is because the study focuses on overall system speed rather than specific control techniques for yaw. This paves the way for future control strategy decisions. Smaller actuators could provide space for weighted coin placement, and different materials may enhance the pendulum's weight.

ACKNOWLEDGEMENT

We wish to express our gratitude to the honorable Universiti Teknikal Malaysia Melaka (UTeM) and the Ministry of Higher Education (MOHE) for sponsoring this work under grant no. PJP/2022/FKE/S01855. Special appreciation and gratitude especially for Universiti Teknologi Malaysia (UTM) KL Campus, Malaysia-Japan International Institute of Technology (MJIIT), Fakulti Teknologi dan Kejuruteraan Elektrik (FTKE) and Underwater Technology Research Group (UTeRG), Center for Robotics and Industrial Automation (CERIA) and Ministry of Higher Education (KPT) for supporting this research.

REFERENCES

[1] L. Shi, S. Su, S. Guo, K. Tang, S. Pan, Y. he, H. Xing, Z. Chen, and P. Guo. (2017) A fuzzy PID control method for the underwater spherical robot. 2017 IEEE International Conference on Mechatronics and Automation (ICMA)., 626–631.

[2] O. Lang (2010). The dangers of mining around the world. *BBC News*, Retrieved from https://www.bbc.com/news/world-latin-america-11533349

[3] Y. Li, M. Yang, H. Sun, Z. Liu, and Y. Zhang. (2018) A Novel Amphibious Spherical Robot Equipped with Flywheel, Pendulum, and Propeller. J. Intell. Robot. Syst., 89(3–4):485–501.

[4] S. Radu (2019). The Top 5 Deadliest Disasters in 2019. U.S.News, Retrieved from https://www.usnews.com/news/best-countries/slideshows/5-of-the-deadliest-natural-disasters-in-2019?slide=6

[5] L. DeMunno (2018). 9 natural disasters that took the lives of hundreds of thousands. Business Insider US, Retrieved from https://www.businessinsider.my/worst-natural-disasters-2018-7/?r=US&IR=T

[6] S. Guo, Y. Liu, L. Shi, P. Guo, H. Xing, X. Hou, Z. Chen, S. Su, and H. Liu. (2018) Binocular Camera-based a Docking System for an Amphibious Spherical Robot. 2018 IEEE International Conference on Mechatronics and Automation (ICMA)., 1621–1626.

[7] G. S. Soh, S. Foong, and K. Wood. (2017) De-coupled dynamics control of a spherical rolling robot for waypoint navigation. 2017 IEEE International Conference on Cybernetics and Intelligent Systems (CIS) and IEEE Conference on Robotics, Automation and Mechatronics (RAM)., 562–567.

[8] A. Nakashima, S. Maruo, R. Nagai, and N. Sakamoto. (2018) 2-Dimensional Dynamical Modeling and Control of Spherical Robot Driven by Inner Car. 2018 IEEE International Conference on Robotics and Biomimetics (ROBIO).,1846–1851.

[9] J. Kim, T. Kim, and S. C. Yu. (2018) Conceptual Design of a Spherical Underwater Vehicle Equipped with Vertically Rotatable Thruster Units. 2018 IEEE/OES Autonomous Underwater Vehicle Workshop (AUV)., 1–4.

[10] M. T. Andani, S. Shahmiri, H. Pourgharibshahi, K. Yousefpour, and M. H. Imani. (2018) Fuzzy-Based Sliding Mode Control and Sliding Mode Control of a Spherical Robot. IECON 2018-44th Annual Conference of the IEEE Industrial Electronics Society., 2534–2539.

[11] J. V. Raj, K. Lashmi, and R. Shanmughasundaram. (2018) Design of a spherical robot with improved stability for planetary exploration. J. Adv. Res. Dyn. Control Syst., 10(3):1001–1005.

[12] S. Guo, Y. He, L. Shi, S. Pan, R. Xiao, K. Tang, and P. Guo. (2018) Modeling and experimental evaluation of an improved amphibious robot with compact structure. Robot. Comput. Integr. Manuf., 51:37–52.

[13] L. Geng, Z. Hu, Y. Lin, R. Yi, and C. Wang. (2015) A new concept spherical underwater robot with high mobility. 2015 IEEE International Conference on Cyber Technology in Automation, Control, and Intelligent Systems (CYBER)., 887–890.

[14] L. Jia, Z. Hu, L. Geng, Y. Yang, and C. Wang. (2016) The concept design of a mobile amphibious spherical robot for underwater operation. 2016 IEEE International Conference on Cyber Technology in Automation, Control, and Intelligent Systems (CYBER)., 411–415.

[15] H. Xing, S. Guo, L. Shi, X. Huo, S. Su, Z. Chen, Y. Liu, and H. Liu. (2018) Performance Evaluation of a Multi-Vectored Water-Jet Propellers Device for an Amphibious Spherical Robot. 2018 IEEE International Conference on Mechatronics and Automation (ICMA)., 1591–1596.

[16] X. Hou, S. Guo, L. Shi, H. Xing, Y. Liu, H. Liu, Y. Hu, D. Xia, and. Z. Li. (2019) Hydrodynamic analysis-based modeling and experimental verification of a new water-jet thruster for an amphibious spherical robot. Sensors, 19 (2): 259.

[17] H. Xing, S. Guo, L. Shi, X. Hou, Y. Liu, and H. Liu. (2019) Design, modeling and experimental evaluation of a legged, multi-vectored water-jet composite driving mechanism for an amphibious spherical robot. Microsyst. Technol., 1–13.

[18] B. Alexey, K. Alexander, K. Yury, and K. Anton. (2019) Stabilization of the motion of a spherical robot using feedbacks. Appl. Math. Model., 69: 583–592.

[19] B. B. Dey and M. Jenkin. (2018) Spherico: rapid prototyping a spherical robot. 2018 IEEE International Conference on Information and Automation (ICIA)., 957–962.

[20] Y. Ping, S. Hanxu, Q. Zhongjiang, and C. Jiazhen. (2016) Design and Motion Control of a Spherical robot with Stereovision. 2016 IEEE 11th Conference on Industrial Electronics and Applications (ICIEA)., 1276–1282.

[21] M. Taheri Andani, Z. Ramezani, S. Moazami, J. Cao, M. M. Arefi, and H. Zargarzadeh. (2018) Observer-Based Sliding Mode Control for Path Tracking of a Spherical Robot. Complexity, 2018:1-15.

[22] Q. Zhan. (2015) Motion planning of a spherical mobile robot. Motion and Operation Planning of Robotic Systems. Springer., 361–381.

[23] S. Gajbhiye and R. N. Banavar. (2016) Geometric modeling and local controllability of a spherical mobile robot actuated by an internal pendulum. Int. J. Robust Nonlinear Control, 26(11):2436–2454.

[24] M. Roozegar, M. Ayati, and M. J. Mahjoob. (2017) Mathematical modelling and control of a nonholonomic spherical robot on a variable-slope inclined plane using terminal sliding mode control. Nonlinear Dyn., 90(2):971–981.

[25] N. Muraleedharan, D. S. Cohen, and D. R. Isenberg. (2016) Omnidirectional locomotion control of a pendulum driven spherical robot. SoutheastCon 2016.,1–6.

[26] S. Asiri, F. Khademianzadeh, A. Monadjemi, and P. Moallem. (2019) The Design and Development of a Dynamic Model of a Low-Power Consumption, Two-Pendulum Spherical Robot. IEEE/ASME Trans. Mechatronics., 24(5): 2406–2415.

[27] K. Landa and A. K. Pilat. (2015) Design and start-up of spherical robot with internal pendulum. 2015 10th International Workshop on Robot Motion and Control (RoMoCo)., 27–32.

[28] K. Landa and A. K. Pilat. (2016) Design of a controller for stabilization of spherical robot's sideway oscillations. 2016 21st International Conference on Methods and Models in Automation and Robotics (MMAR).,484–489.

[29] I. Ciufolini and J. A. Wheeler. (1995) Gravitation and inertia, Princeton university press., 101.

[30] S. Lindström. (2019) Lectures on engineering mechanics: statics and dynamics.

[31] M. B. Bahar, S. S. Abdullah, M. S. M. Aras, N. F. Ibrahimjee, F. N. Zohedi, M. H. Harun, A. A. Yusof, and M. K. Aripin. (2022) A Spherical Amphibian Underwater Robot: Preliminary Mechanical Design. 2022 IEEE 9th International Conference on Underwater System Technology: Theory and Applications (USYS)., 1–6.

[32] M. B. Bahar, S. S. Abdullah, M. S. M. Aras, and F. N. Zohedi. (2022) Spherical Amphibian Robot Design with Novel Driving Principle. Proceedings of the 12th National Technical Seminar on Unmanned System Technology 2020., 69–77.